UC Berkeley
UC Berkeley Previously Published Works

Title

A new continuum model of the incoherent interface compared with growth of a spinel rim on an olivine grain

Permalink

https://escholarship.org/uc/item/71f9j9mv

Author

Morris, SJS

Publication Date

2019-07-01

DOI

10.1016/j.pepi.2019.03.001

Peer reviewed

eScholarship.org Powered by the California Digital Library
University of California

Significance of the incoherent interface for modelling of the olivine–spinel transformation

S. J. S. Morris[a]

[a]*Department of Mechanical Engineering, University of California Berkeley, CA 94720, USA*

Abstract

We compare two models of growth of a rim of high–pressure phase on a sphere which is initially at uniform pressure p_0, and whose surface is kept at that pressure. The models share these features: the same thermodynamic potential is used to describe the effect of strain energy on interface kinetics; stress–free strain enters only into the relation between pressure within an element of product phase, and the volume strain experienced by it from its initial state as parent phase; at the interface, the normal component of displacement is continuous, and the shear stress vanishes. The models differ in one respect. In one, deviatoric stress within an element of product is determined by the total deviatoric strain from the initial state. In the other, deviatoric stress is determined by the increment in deviatoric strain subsequent to transformation; memory of prior deviatoric strain is erased within the incoherent interface as the lattice is rebuilt. The first model is not consistent with experiments on the olivine–ringwoodite transformation in single crystals: it predicts that samples should have transformed completely at a roughly constant rate; instead, growth slowed, and may even have ceased. The second model predicts this behaviour: evem with purely elastic deformation, theory and experiment agree adequately for samples having 75–200 ppmw of water. For nominally anhydrous samples, rims are thinner than predicted. As creep is not essential to this model, these very thin rims suggest water may be essential to lattice reconstruction.

1. Introduction

With increasing pressure, olivine, the chief constituent of earth's upper mantle, undergoes a series of densification phase changes, first to a modified spinel structure (wadsleyite), then to the spinel structure (ringwoodite). Deviatoric stress so generated has been proposed as a cause for deep earthquakes within subducting oceanic plates (Brudzinski and Chen 2005). Morris (2017, p.256) shows that, although existing models predict that the volume reduction generates a deviatoric stress ∼GPa, the predicted magnitude is an artefact of the modelling assumptions. Those models do not account for microstructure: compaction occurs at the grain scale, and produces a large deviatoric stress at that

scale. The mechanism by which devatoric stress at the grain scale produces deviatoric stress at the seismic scale is not understood. However, the grain–scale is accessible experimentally, and, if the physics at that scale were understood, the behaviour of polycrystals could be treated by computation. There are two major problems: accounting for the sensitivity of the phase change to traces of hydrogen (water), and formulating a constitutive relation for the product.

We show here that experiments on single crystals can illuminate both problems. In these experiments, a sphere or cube cut from a single crystal of San Carlos olivine is raised to the desired pressure and (then) temperature within the stability field of the spinel structure. Product nucleates rapidly to form a continuous rim, which then grows at the expense of the olivine (Kubo et al. 1998a,b; Liu et al. 1998; Mosenfelder et al. 2000; Diedrich et al. 2009; Du Frane et al. 2013). Growth is sensitive to water. At 18 GPa and 1373 K, a 0.5 mm sphere with initial water concentration of ~ 300 ppmw transformed completely in about 1 hour (my estimate); however, after 3 hours at those conditions, the rim on a sphere of nominally anhydrous olivine was only 17 μm thick (Diedrich et al. 2009, table 1). Because the phases differ in specific volume (inverse of the density), growth of the rim implies the presence of deviatoric strain within the rim. Deviatoric strain will cause a deviatoric stress, whose magnitude will depend on the rheology of the rim. Though the rheology is poorly known, observations of dislocation microstructure are consistent with the presence of deviatoric stress within the rim. They also suggest that water facilitates creep within the rim (Kubo et al. 1998a,b). However, Mosenfelder et al. (2001, p.169) have stressed that water may also affect interface kinetics. Theory is needed to disentangle those alternatives.

This brings us to the second problem: formulating the constitutive relation. Because the sample initially consists of olivine alone, all material within the rim has been processed by passing through the thin interphase region. The constitutive relation for the product might be expected to depend on the nature of that region. In these experiments, no preferred crystallographic orientation is observed between the product rim and the olivine core; such interfaces[1] are described as being incoherent (Kerschhofer et al. 1998, Kubo et al. 1998b, Mosenfelder et al. 2000). But, unlike the term coherent interface, whose implications are precisely defined by the condition that the lattice (and so the displacement vector) are continuous across it, the absence of preferred orientation does not determine the corresponding physical model.

Here, we analyse two constitutive models. In the first (existing) model, stress is assumed to be uniquely determined by the total strain from the initial state, independent of the path taken to reach the current state (Larché and Cahn 1973, p.1056; Larché and Cahn 1985, §4.1). The incoherent interface is assumed to differ from a coherent interface only in the boundary condition imposed upon

[1] In this work, 'incoherent' refers only to the interface. The word is also used to describe a particle of precipitate within which all deviatoric stress has been relaxed (Christian 1965, p.416; Lee and Johnson 1978; Mura 1987, pp. 226, 417).

the tangential component of displacement. At a coherent interface, the displacement vector is continuous; at an incoherent interface, the normal component of displacement is continuous, and free slip is allowed along the interface (Nabarro 1940; Larché and Cahn 1978, equation 25). For spherically–symmetric growth, slip is absent and the distinction between coherent and incoherent interfaces is lost (Christian 1965, p. 416).

To show the implication of path–independence, we note that when an olivine sphere is transforming to ringwoodite, a material element within the rim initially consisted of olivine at uniform pressure p_0, and currently consists of ringwoodite in a certain state of deviatoric strain. Suppose that the element was first transformed, without deviatoric strain, to ringwoodite at uniform pressure p_0; then, as ringwoodite, deformed into its current state of deviatoric strain. If the deviatoric stress is independent of path, the same deviatoric stress will result if the element is first deformed into its current state of deviatoric strain, then transformed to ringwoodite without further deviatoric strain. But, if there is no relation between the lattices, the lattice within that very element must have been rebuilt as the interface passed over it. One might expect that to erase the memory of deviatoric strain suffered by the element before, or during, its transformation.

This idea is consistent with physical picture of the incoherent interface given in the literature. Of nucleation and growth, Christian (1965) writes: 'individual atoms move independently, there is no correlation between the initial and final positions of the atoms after retransforming to the original phase.' (p.12)... 'In some nucleation and growth transformations in the solid state, there is no relation between the orientations of the two lattices.' (p.13) Those passages imply that if the interface is incoherent, individual atoms cross it independently. Likewise, Sung and Burns (1978, p.192) write that 'the original olivine structure disintegrates ... the migration of atoms across the interfaces to join spinel nuclei may not follow a definite path but may be achieved by a complicated process of random walk.' By developing a continuum model incorporating the idea that the lattice is rebuilt, we test that atomistic picture.

With this motivation, in the new model, we assume that, within a material element, deviatoric stress depends only on the increment in deviatoric strain since the element was transformed. For the first time, the distinction between coherent, and incoherent, interfaces is retained for spherical–symmetric growth.

In §2, §3 the problem is stated, and the new constitutive relation is formulated. In §4, we state those properties of spherically symmetric deformation which are independent of the constitutive assumption; these results are used to simplify analysis of the models discussed here. In §5, the interface kinetic relation is described. The rate parameter λ (ratio of interface speed to potential difference driving propagation) is assumed to be independent of time.

In §6, the existing model is analysed. The treatment differs from that in Morris (2014), because it is organized about the aim of showing that the two models can be distinguished experimentally. To this end, compressibility of the phases is included here. The analysis predicts the existence of a threshold for the applied pressure p_0. Below the threshold no product forms; above it, transfor-

mation should occur at a rate which is, roughly speaking, independent of time. (Broadly similar behaviour is found for elastic, and for elastic perfectly plastic, bodies.) That prediction is not consistent with experiment: near but above the coexistence (Clapeyron) curve, Kubo et al. (1998b; 1303 K, 13.5 GPa) observe a well–defined product rim; well above the coexistence curve (Mosenfelder et al. 2000; 1373 K, 17 GPa) observe an interface velocity which decreases with time. Though water is preferentially partitioned into the high–pressure phases (wadsleyite, ringwoodite), this might be expected to enhance plastic deformation within the rim, but also, by removing water from the interface, inhibit the reaction occurring there (Mosenfelder et al. 2001). There seems to be be no simple way to reconcile existing theory with experiment.

The new model is analysed in §7. It predicts behaviour consistent with observation. Whenever the applied pressure p_0 exceeds the Clapeyron pressure $\bar{p}$ at which the phases would coexist in a common hydrostatic state, a product rim grows at a rate which decreases with time. This leads to a state in which the rim and the core of parent olivine coexist on the laboratory time scale. The thickness of this equilibrium rim vanishes for $p_0 = \bar{p}$, and increases with excess pressure $p_0 - \bar{p}$.

In §8, experiment and theory are compared in detail. For purely elastic deformation, the new theory contains no adjustable constants: in this simple form, it agrees adequately with experiments on samples containing 75–200 ppmw of water. For nominally anhydrous (< 6 ppmw of water) samples, however, the new model predicts much thicker rims than observed. This could be explained if the rate parameter λ decreased with time for the drier samples. Predictions are relatively insensitive to plastic deformation.

As for conditions in the oceanic lithosphere, Peslier and Bizimis (2015, table 1) report a bulk water content of only 45 ppmw in a peridotite xenolith from the Pali vent on O'ahu, Hawaii; they argue that this sample is representative of unmetasomatized Pacific lithosphere. If water is essential to the reconstructive process occurring at the phase interface in the single crystal experiments, and also to the competing process of intracrystalline growth, deciding whether metastable olivine can exist within subducting slabs will require further experiments showing the behaviour as a function of water content in the range 5–50 ppmw. If, at low water fractions, the reconstructive process is water–limited, the size of a metastable wedge could be controlled by mass transfer within the oceanic lithosphere.

Better experiments are needed for a more exacting test of the new theory. Because drier samples tend to gain water over long times, determining large–time behaviour may require extrapolation; this will be more reliable if scatter is reduced, a sufficient number of data are acquired, and measurements are repeated by independent groups. The new theory will have served its purpose if attempts to falsify it lead to systematic measurements of rim thickness as a function of time and thermodynamic state.

2. Formulation

For an arbitrary tensor t_{ij}, its deviator $t'_{ij} = t_{ij} - \frac{1}{3}t_{kk}\delta_{ij}$. The summation convention applies, and δ_{ij} denotes the unit tensor.

In the initial (reference) state, the sample consists of parent phase at uniform pressure p_0. A subscript '0' denotes a variable evaluated in this uniform state. According to Morris (2014, p.131), rim growth causes a strain which is of the order of the fractional difference in specific volume between the phases. Because that difference is less than 7% for the olivine–ringwoodite transformation, we assume infinitesimal strain.

The infinitesimal strain tensor e_{ij} is defined in terms of the displacement u_i of a material element from its position in the initial state:

$$e_{ij} = \frac{1}{2}\Big(\frac{\partial u_i}{\partial x_j} + \frac{\partial u_j}{\partial x_i}\Big). \tag{1}$$

For the initial state, the stress tensor is $-p_0\delta_{ij}$. The tensor σ_{ij} represents the additional stress caused by rim growth. Quantities representing absolute stresses are denoted by a tilde. Pressure is defined as the negative of the mean normal stress: the relative pressure $p = -\frac{1}{3}\sigma_{kk}$ and the absolute pressure $\tilde{p} = p_0 + p$. In this notation,

$$\tilde{\sigma}_{ij} = -\{p + p_0\}\delta_{ij} + \sigma'_{ij}. \tag{2}$$

3. Constitutive relation

Because the conduction time is of the order a few seconds for the mm–sized samples used in the experiments, we assume the process to be isothermal. In an elastic material, the thermodynamic state of a material element is then uniquely specified by the phase, and the components e_{ij} of the deformation tensor. In particular, σ_{ij} depends on e_{ij}, and on the phase. The two constitutive models differ in the relation assumed for deviatoric stress, but have the same relation for pressure.

3.1. Mean normal stress

We assume that, within a phase, specific volume $V = 1/\rho$ and relative pressure satisfy

$$V = V_0\{1 - \kappa p\}\,; \tag{3}$$

The compressibility κ is evaluated at the initial pressure p_0; V_0 denotes the specific volume of the phase at pressure p_0. For the experiments at issue, the linear approximation (3) is satisfactory because κp is typically small.

Because the equation of equilibrium refers to a material element, we express (3) in terms of $\boldsymbol{u}$. A material element which has been converted into product phase 2 began as parent phase 1 at the reference pressure p_0 with specific volume V_{10}. In its current state, it is at pressure p with specific volume $V_2(p)$. The change in its specific volume is

$$V_2(p) - V_{10} = \{V_2(p) - V_{20}\} + \{V_{20} - V_{10}\}.$$

According to the theory of infinitesimal strain, $V_2(p) - V_{10} = V_{10}\,\mathrm{div}\,\boldsymbol{u}$. On the right hand side, the first term contains only properties of a single phase: it is given by (3) with the appropriate value of κ. The remaining term $V_{20} - V_{10}$ represents the difference in specific volumes of the phases in the initial state.

Let

$$\theta_0 = \frac{V_{20} - V_{10}}{V_{10}}. \tag{4a}$$

In the terminology used by Eshelby (1961, p.91), the tensor $e_{0ij} = \frac{1}{3}\theta_0\delta_{ij}$ defines the 'stress–free' or 'transformation' strain. Also let

$$\theta = \mathrm{div}\ \boldsymbol{u}. \tag{4b}$$

Then, dilatation θ and relative pressure p satisfy

$$\theta = \begin{cases} \theta_0 - \kappa_2\, p & \text{(product)}, \\ -\kappa_1\, p & \text{(parent)}. \end{cases} \tag{5a, b}$$

Consistent with the small strain assumption, in (5a), a factor V_{20}/V_{10} multiplying p has been set to unity. Equation (5) holds for both constitutive models.

3.2. Deviatoric stress

3.2.1. Existing model

Within both parent and product, the deviatoric stress tensor σ'_{ij} and deviatoric strain tensor e'_{ij} satisfy Hooke's law:

$$\sigma'_{ij} = 2\mu e'_{ij}, \tag{6}$$

with the appropriate value of μ. The constitutive relation consisting of (5) and (6) is analogous to the Duhamel–Neumann law in thermoelasticity; compare Larché and Cahn (1985, equation 4.2) with Sokolnikoff 1956, equation 99.4).

In writing (6), we imply that, even though the lattice is reconstructed, deviatoric stress within an element of product depends on the total deviatoric strain experienced by that element from its initial state as olivine. Though this assumption is reasonable for a coherent interface, it can hardly be correct when the interface is incoherent, and the lattice is rebuilt. By eliminating this assumption from the new model, we examine its implications.

3.2.2. New model

We assume that the crystal lattice is rebuilt, and that, while an element of the solid is in that incoherent state, all memory of deviatoric strain experienced by the element before, or during, its transformation is erased. As a result, within the product, deviatoric stress within an element of material depends only on the deviatoric strain experienced by that element since its transformation.

Let τ denote the time at which the material element at position $\boldsymbol{x}$ is transformed. Also $e'_{2ij}(\boldsymbol{x}, \tau)$ denote the strain evaluated within the product so formed; because the deviatoric strain proves to be discontinuous across the interface, the subscript 2 is used to indicate the phase to be used. (Strain is,

of course, calculated using (1), and the unique reference state already defined.) Then,

$$\sigma'_{ij}(\boldsymbol{x},t) = \begin{cases} 2\mu_2\big\{e'_{2ij}(\boldsymbol{x},t) - e'_{2ij}(\boldsymbol{x},\tau)\big\} & t > \tau, \\ 2\mu_1 e'_{1ij}(\boldsymbol{x},t) & t < \tau. \end{cases} \qquad (7a,b)$$

If $\boldsymbol{x}$ is now taken to approach the interface from the product side, $\tau \to t$, and (7a) implies that σ'_{ij} vanishes within the product at the interface. This leads to the boundary conditions at the interface.

Let n_i, $\{u_{1i}, \sigma_{1ij}\}$ and $\{u_{2i}, \sigma_{2ij}\}$ denote, respectively, the unit normal to the interface, and the displacement vector and stress tensor at the interface within the phase indicated as 1 or 2. Then, at the interface,

$$(u_{2i} - u_{1i})n_i = 0, \qquad (8a)$$

$$\sigma_{1ij}n_j = \sigma_{2kl}n_k n_l\, n_i. \qquad (8b)$$

According to (8a), the phases remain in contact, but do not overlap. This condition can be obtained by integrating the finite quantity div $\boldsymbol{u}$ over an infinitesimal volume spanning the interface, then using the divergence theorem. Next, (8b) follows from (7) and the usual condition of continuity of $\sigma_{ij}n_j$; together, these require the stress vector within the parent 1 to be perpendicular to the interface.

In the existing model, coherent and incoherent interfaces differ only because there is no–slip along a coherent interface; along an incoherent interface, phases slip freely, and the shear stress vanishes. (Larché and Cahn 1985, p.332). For spherically symmetric growth, symmetry excludes slip, and the distinction between the two types of interface disappears. In the new model, the distinction is retained even then.

Plastic deformation is included in the usual way, as detailed when needed. By using the elastic–plastic rheology, we only account for inelastic deformation on the single time scale imposed through interface kinetics. Longer time scales may be set, for example, by diffusion of water, or by creep.

4. Properties of spherically symmetric growth

In experiments on single spheres machined from single crystal olivine, the phase interface remains approximately spherical (Mosenfelder et al. 2001, figure 2). Because there is no evidence for any instability, we now specialize to spherically symmetric growth.

Fig.1 shows the geometry of the problem to be analysed. Parent phase of compressibility κ_1 occupies the central sphere; product of rigidity μ and compressibility κ_2 occupies the annular rim $R(t) < r \leq b$. The object is to predict $R(t)$. Because $|\theta_0| \ll 1$, sample radius b can be taken as constant throughout the entire transformation. The displacement field is $\boldsymbol{u} = u(r)\mathbf{e}_r$.

For the special case $\kappa_1 = 0 = \kappa_2$ of incompressible phases, expressions given here for the strain for arbitrary κ reduce to those in Morris (2014). Other expressions in that work are the special cases, for zero compressibility, of results given here for the existing model.

The following properties are independent of the constitutive assumption.

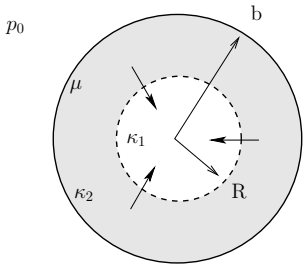

Figure 1: Product rim (rigidity μ, compressibility κ_2) consuming the parent (compressibility κ_1). Phase interface radius $R(t)$; sample radius b.

4.1. Strain compatibility and its implications

Boundary condition (8a) is equivalent to the following condition of strain compatibility:

$$e_{rr}(R^+) - e_{rr}(R^-) = \theta(R^+) - \theta(R^-). \tag{9}$$

This follows by evaluating the identity $\theta = e_{rr} + 2u/r$ on each side of the interface, then equating the results. With (8a) now incorporated, we need not consider u further.

As it is transformed, a material element suffers a discontinuous deviatoric strain: by (9), because $e'_{rr} = 0$ for $r < R(t)$,

$$\tfrac{3}{2}e'_{rr}(R^+) = \theta(R^+) - \theta(R^-). \tag{10}$$

The identity $e_{rr} = e'_{rr} + \frac{1}{3}\theta$ has been used. (That $e'_{rr} = 0$ for $r < R$ is proved below (12); (10) is not used there.) Equation (10) is the basis of the distinction between the two models considered here.

4.2. Properties involving the stress

Owing to spherical symmetry, the deformation tensor is diagonal when expressed in spherical polar coordinates $\{r, \theta, \phi\}$. (In this paragraph, only, θ denotes a coordinate, rather than the dilatation.) The stress tensor, too, is diagonal: the principal axes of stress and strain coincide because the material is isotropic; and the displacement, purely radial. The non–zero stress components are $\sigma_{rr} = -p + \sigma'_{rr}$ and $\sigma_{\theta\theta} = \sigma_{\phi\phi} = -p - \frac{1}{2}\sigma'_{rr}$; all depend only on r. The circumferential components of the equations of equilibrium are satisfied identically; the radial component is

$$0 = r^3\frac{\mathrm{d}\sigma_{rr}}{\mathrm{d}r} + 3r^2\sigma'_{rr} = -r^3\frac{\mathrm{d}p}{\mathrm{d}r} + \frac{\mathrm{d}(r^3\sigma'_{rr})}{\mathrm{d}r}. \tag{11a,b}$$

The conditions of mass conservation and mechanical equilibrium together require that

$$\frac{3}{2}e'_{rr} + \kappa\sigma'_{rr} = \frac{C(t)}{r^3}, \tag{12}$$

with $C(t)$ an arbitrary function (Morris 1995, equation 3.2). Equation (12) follows by integrating the equation obtained by using the identity

$$r^3 \frac{\mathrm{d}\theta}{\mathrm{d}r} = \frac{3}{2} \frac{\mathrm{d}}{\mathrm{d}r}(r^3 e'_{rr})$$

to eliminate p between (11b) and the equation of state (5).

Because, owing to the phase change, the form taken by (5) differs within the core, and product rim, the function $C(t)$ is evaluated separately for core and rim. (It is consistent with this logic, that in §6.2.1, where we consider plasticity, we take $C(t)$ to be identical on either side of the yield surface: no change of phase occurs there.)

Within the core, $C(t) = 0$ because e'_{rr} and σ'_{rr} are finite at $r = 0$. Then, (12) requires that $\frac{3}{2}e'_{rr} + \kappa\sigma'_{rr} = 0$. Because we are concerned with growth of a rim of product into the core of parent, the distinction between constitutive models affects only the rim. Within the core, Hooke's law applies for either model: so, $e'_{rr} = 0 = \sigma'_{rr}$, and p is uniform by (11b). Let this uniform pressure be $p_1(t)$.

Within the rim, $C(t) = \{\theta_0 + (\kappa_1 - \kappa_2)p_1(t)\}R^3$, and

$$\frac{3}{2}e'_{rr} + \kappa_2\sigma'_{rr} = \big\{\theta_0 + (\kappa_1 - \kappa_2)p_1(t)\big\}\frac{R^3}{r^3}. \tag{13}$$

The equation for $C(t)$ follows by setting $r = R$ in (12), then substituting the relation obtained by eliminating θ between (5) and (10), and imposing continuity of the normal stress. In (13), terms in braces represent the sources of deviatoric stress. These are the difference between the specific volumes of the phases, and differential contraction owing to their differing compressibilities.

The uniform core pressure is given by

$$p_1(t) = -3\int_R^b \sigma'_{rr}\frac{\mathrm{d}r}{r}. \tag{14}$$

This follows by integrating (11a) from $r = R$ to $r = b$, using continuity of the normal stress, and imposing the condition $\sigma_{rr}(b) = 0$.

In this formulation, core pressure p_1 is determined as a function of interface radius R by (13), (14) and the constitutive relation. To complete the formulation, interface kinetics must be included.

5. Interface kinetics

Let F and $\tilde{\sigma}_{nn} = p_0 + \sigma_{nn}$ denote the Helmholtz function (isothermal strain energy) per unit mass, and absolute normal stress $\tilde{\sigma}_{ij}n_in_j$; as previously defined, n_i denotes the unit normal to the interface. Also let $\Phi = F - V\tilde{\sigma}_{nn}$.

Then, provided the shear stress vanishes on the interface, the mass flux J across the interface from phase 1 into phase 2 satisfies

$$J\{\Phi_1 - \Phi_2\} > 0 : \tag{15}$$

the phase having the higher potential converts into that having the lower potential (Vaughan et al. 1984; see also Morris 2017, §5). Equivalently, phase 1 converts into phase 2 if, and only if,

$$V_2\tilde{\sigma}_{2nn} - V_1\tilde{\sigma}_{1nn} > F_2 - F_1 :$$

a particle of phase 1 converts into phase 2 if the compression work performed on it during transformation exceeds the increase in its strain energy. Compression work drives transformation; storage of free energy impedes it. Because deviatoric stress influences both effects, it can either inhibit, or promote, transformation (Morris 2014, above equation 25).

Because (15) is to be satisfied for an arbitrary transformation, J must be a function of $\Phi_1 - \Phi_2$ having the same sign as $\Phi_1 - \Phi_2$. Consequently, J must vanish when $\Phi_1 - \Phi_2 = 0$. Because the existing model can be distinguished from the new model by comparing their predictions of when transformation starts, and stops, it is sufficient to assume the linear relation $J \propto \Phi_1 - \Phi_2$. By (15), the constant of proportionality is positive.

J is related to the interface speed $\dot{R} = \mathrm{d}R/\mathrm{d}t$, and to the velocity v and density ρ of the material by $J = \rho_1\{v_1 - \dot{R}\}$. This can be replaced by $J = \rho_1\dot{R}$, because v_1 proves to be smaller than $\dot{R}$ by a factor $\sim |\theta_0| \ll 1$. Hence, by (15),

$$\frac{\mathrm{d}R}{\mathrm{d}t} = -\lambda\{\Phi_1 - \Phi_2\}. \tag{16}$$

The potential Φ is evaluated at the interface, on the side indicated by the subscript. The rate parameter λ is non–negative, by the remark ending the previous paragraph. Equation (16) is written so as to make it clear that a rim of phase 2 (spinel) grows into the core of phase 1 (olivine) if phase 1 is at a higher potential than phase 2.

We assume λ to be independent of time.

For spherically–symmetric deformation, $\tilde{\sigma}_{nn} = \tilde{\sigma}_{rr}$. As already shown in §4, within the core, the stress is hydrostatic, $\tilde{\sigma}_{1rr} = \tilde{\sigma}_{\theta\theta} = \tilde{\sigma}_{\phi\phi} = -\tilde{p}_1$, and continuity of the normal stress across the interface requires that $\tilde{\sigma}_{2rr} = -\tilde{p}_1$. So $\Phi = F + \tilde{p}_1 V$, and

$$\Phi_2 - \Phi_1 = \{F_2 + \tilde{p}_1 V_2(\tilde{p}_2)\} - \{F_1 + \tilde{p}_1 V_1(\tilde{p}_1)\}. \tag{17}$$

In (17), F and V are evaluated for the thermodynamic state appropriate to the side of the interface on which phase exists. The terms $\tilde{p}_1 V_2(\tilde{p}_2)$ and $\tilde{p}_1 V_1(\tilde{p}_1)$ are evaluated using the equation of state in the form (3). As for the function of state F, it is a property of a given polymorph at given stress and temperature. Consequently, the formula for it differs from the usual expression for a single phase only because, here, we must incorporate the initial pressure p_0.

Because the process is isothermal,

$$\mathrm{d}F = V_0\tilde{\sigma}_{ij}\mathrm{d}e_{ij}, = -\{p_0 + p\}\,\mathrm{d}V + V_0\sigma'_{ij}\mathrm{d}e'_{ij}. \tag{18a,b}$$

Equation (2) has been used. We must now specialize to a particular model.

6. Existing model

6.1. Elastic solid

6.1.1. Stress

By eliminating e'_{rr} between Hooke's law (6), and (13)

$$(\kappa_2 + \tfrac{3}{4}\mu^{-1})\sigma'_{rr} = \{\theta_0 + (\kappa_1 - \kappa_2)p_1(t)\}\frac{R^3}{r^3}. \tag{19}$$

Together, (19) and (14) determine the pressure $p_1(t)$ within the core, and the radial deviatoric stress $\sigma'_{rr}(r,t)$ with the product rim.

Let

$$k_{\rm m} = \frac{|\theta_0|}{\kappa_2 + \frac{3}{4}\mu^{-1}}, \tag{20a}$$

$$\varepsilon = \frac{\kappa_2 - \kappa_1}{\kappa_2 + \frac{3}{4}\mu^{-1}}; \tag{20b}$$

$k_{\rm m}$ is a measure of the stress caused by the volume difference between the phases. ε controls the magnitude of the differential contraction which occurs when the phases differ in compressibility; $-\infty < \varepsilon < 1$.

Then,

$$p_1 = -\frac{k_{\rm m} f_2}{1 - \varepsilon f_2}\,\mathrm{sgn}\ \theta_0, \tag{21a}$$

$$\sigma'_{rr} = \frac{k_{\rm m}}{1 - \varepsilon f_2}\frac{R^3}{r^3}\,\mathrm{sgn}\ \theta_0, \tag{21b}$$

$f_2 = 1 - R^3/b^3$ denotes the volume fraction of product. Equation (21) is equivalent to a result by Lee and Tromp (1995).

It is instructive to compare the physical motivation of the two analyses. Lee and Tromp determine the stress within a composite sphere comprising shells of different materials. The shell radii are given constants and the composite is initially stress–free. Lee and Tromp were motivated by the process of metamictization: in a mineral containing radioactive elements, their decay can cause the crystalline structure to become amorphous (metamict). In their model, amorphization and the change in specific volume are assumed to occur sequentially. In the present problem, the processes are not sequential. As the interface propagates over it, a material element changes phase; simultaneously, the lattice is rebuilt, and the element experiences the discontinuity in deviatoric strain. In using the existing model, we implicitly assume that this rapid increase occurs within the product, instead of within the thin interphase layer.

Compressibility weakens the effect of deviatoric stress: as $\kappa_2 \to \infty$ (increasing compressibility), $k_{\rm m} \to 0$ and σ'_{rr} and p_1 both vanish, as if μ were zero. We also note that for $\theta_0 < 0$ (dense rim), $p_1 > 0$ and $\sigma'_{rr} < 0$; also, p_1 vanishes initially (when $f_2 = 0$) and increases roughly linearly with volume fraction of product f_2, but σ'_{rr} is non–zero whenever any product is present. These results can be understood using (13) for the special case $\kappa_1 = 0 = \kappa_2$; then $\varepsilon = 0$.

Because Hooke's law (6) requires σ'_{rr} and e'_{rr} to have the same sign, (13) requires σ'_{rr} to have the same sign as θ_0: radial deviatoric stress with a rim of dense elastic product is negative (compressive). The condition of mechanical equilibrium (14) then requires $p_1 > 0$: the absolute pressure within the core of remnant olivine exceeds the applied pressure. Though this effect of deviatoric stress proves to promote, rather than to inhibit, transformation in an elastic body, we now show that storage of strain energy acts in the opposite sense.

6.1.2. Potential

Let F_0 denote the Helmholtz function for the initial hydrostatic state p_0. By integrating (18b), we obtain

$$F = F_0 + \kappa V_0\, p_0\, p + \tfrac{1}{2} V_0 \{\kappa p^2 + \tfrac{3}{4}\mu^{-1}(\sigma'_{rr})^2\}. \tag{22}$$

This equation expresses F as the sum of a contribution from the externally applied pressure p_0, and additional terms due to stress internal to the sample grain. The term linear in the relative pressure p describes work done by the initial pressure p_0 as the specific volume V changes owing to the internal pressure. Quadratic terms (in braces) describe work done by the internal stress in compressing and deforming the material element; these terms correspond to the usual expression giving F for an elastic body deformed from a state of zero initial stress (Fung 1965, §12.8). Let $G_0 = F_0 + p_0 V_0$ denote the usual Gibbs function evaluated in the hydrostatic initial state. Also let $[G_0]_1^2 = G_{20} - G_{10}$, and let $[V_0]_1^2 = V_{20} - V_{10}$. (Larché (1990, p.84) calls $[G_0]_1^2$ the 'chemical free energy'.) Then, $\Phi_2 - \Phi_1$ is given in terms of the relative pressure p_1 within the core, and the deviatoric stress σ'_{rr} within the rim at the interface as follows:

$$\Phi_2 - \Phi_1 = \Big\{ [G_0]_1^2 + [V_0]_1^2\, p_1 - \tfrac{1}{2}[\kappa V_0]_1^2\, p_1^2 \Big\} + \tfrac{1}{2} V_{20}\big(\kappa_2 + \tfrac{3}{4}\mu^{-1}\big)(\sigma'_{rr})^2. \tag{23}$$

Because deviatoric strain is proportional to θ_0, (23) is accurate to the order of θ_0^2. To the same order of accuracy, we may set $V_{10} = V_{20}, = V_0$ in the coefficients of p_1^2 and $(\sigma'_{rr})^2$. In this approximation, $\theta_0 = [V_0]_1^2/V_0$, and

$$\Phi_2 - \Phi_1 = \Big\{ [G_0]_1^2 + V_0\theta_0\, p_1 - \tfrac{1}{2} V_0(\kappa_2 - \kappa_1)\, p_1^2 \Big\} + \tfrac{1}{2} V_0\big(\kappa_2 + \tfrac{3}{4}\mu^{-1}\big)(\sigma'_{rr})^2. \tag{24}$$

Because rim thickness increases if $\Phi_2 < \Phi_1$, the sign of each term in (23) determines whether it represents an impediment, or a cause, of growth. The term proportional to $(\sigma'_{rr})^2$ represents an impediment. Because σ'_{rr} is independent of $[G_0]_1^2$, so is the magnitude of this impedance.

The cause of growth, by contrast, increases with the magnitude of $[G_0]_1^2$. In (23), this cause is represented by the term in braces. To interpret it, we note that within the core, the stress is hydrostatic, $\tilde{\sigma}_{ij} = -\tilde{p}_1 \delta_{ij}$. For this state, the Gibbs function $G(\tilde{p}_1)$ is defined for each phase; the term in braces is the Taylor expansion of the difference $G_2(\tilde{p}_1) - G_1(\tilde{p}_1)$ about $\tilde{p}_1 = p_0$, and, as such, depends on p_0 only through the Taylor coefficients. For transformation to be possible, phase 2 must have smaller Gibbs free energy than phase 1 in the initial

state: $[G_0]_1^2$ must be negative. The next term, $[V_0]_1^2\, p_1$, is negative because p_1 is proportional to $-\theta_0$: because the linear term tends to make $G_2(\tilde{p}_1) - G_1(\tilde{p}_1)$ more negative, it represents an effect promoting growth. The final, quadratic, term modifies this tendency without eliminating it.

This leads to an essential conclusion. Because the magnitude of the impeding term is independent of $[G_0]_1^2$, this term will become negligibly small in experiments performed sufficiently far from the equilibrium boundary. The difference in Gibbs energies in the initial state is then so large as to overwhelm the impeding effect of strain energy. A similar result holds when plasticity is included. This effect does not seem to have been recognized before.

6.2. Elastic perfectly plastic solid

6.2.1. Stress

For spherical symmetry, the von Mises yield criterion requires that $(\sigma'_{rr})^2 = k^2$; the yield parameter k is related to stress difference by $|\sigma_{rr} - \sigma_{\theta\theta}| = \frac{3}{2}k$. Because k is non–negative, σ'_{rr} is related to radial deviatoric strain rate $\dot{\gamma}$ by

$$\sigma'_{rr} = k\ \mathrm{sgn}\,\dot{\gamma}\ . \tag{25}$$

The factor sgn $\dot{\gamma}$ ensures that the dissipation–rate is non–negative.

According to (21), $|\sigma'_{rr}|$ attains its maximum at the phase interface; because there, $|\sigma'_{rr}| = k_{\mathrm{m}}/(1 - \varepsilon f_2)$, deformation is plastic at the interface if

$$(1 - \varepsilon f_2)k \leq k_{\mathrm{m}}. \tag{26}$$

Initially, $f_2 = 0$ and (26) is satisfied if $k \leq k_{\mathrm{m}}$.

For $k < k_{\mathrm{m}}$, deformation is plastic within an inner shell $R < r < c$, and elastic for $r > c$. The elastic region lies outside the plastic region because, in the existing model, the magnitude of σ'_{rr} decreases with increasing distance from the phase interface. Within the elastic region, Hooke's law (6) applies; with (13), it requires that

$$\sigma'_{rr} = \begin{cases} (k_{\mathrm{m}}\mathrm{sgn}\ \theta_0 - \varepsilon p_1)\frac{R^3}{r^3}, & r > c\,; \\ k\ \mathrm{sgn}\,\dot{\gamma}, & R < r < c. \end{cases} \tag{27a, b}$$

The core pressure $p_1(t)$ is determined next.

The boundary condition at the outer surface of the sample grain is imposed when (27) is used to evaluate the pressure integral (14). There are two cases, according as $c \gtrless b$.

Let

$$k_* = \frac{k}{k_{\mathrm{m}}}, \tag{28}$$

where k_{m} is defined by (20). Also, let $f_1 = R^3/b^3$ denote the volume fraction of parent olivine. Then,

$$\frac{p_1}{k} = \ \mathrm{sgn}\,\dot{\gamma}\ \ln f_1, \qquad \text{for } c > b\,; \tag{29a}$$

$$\frac{p_1}{k} = -\Big\{ \ln\Big(\frac{c^3}{R^3}\Big)\ \operatorname{sgn}\dot\gamma + \frac{1}{k*}\Big(\frac{R^3}{c^3} - f_1\Big)\operatorname{sgn}\,\theta_0\Big\}\Big/\Big\{1 - \varepsilon\Big(\frac{R^3}{c^3} - f_1\Big)\Big\}, \quad (29b)$$

for $c < b$.

To determine the radius c of the yield surface, we need the stress within the elastic region $c < r < b$. It is determined by (27a), where p_1 is given by (29b) because $c < b$. On eliminating p_1 between those equations, then rearranging, we obtain

$$\frac{\sigma'_{rr}}{k}\frac{r^3}{R^3}\Big\{1 - \varepsilon\Big(\frac{R^3}{c^3} - f_1\Big)\Big\} = \frac{1}{k_*}\operatorname{sgn}\,\theta_0 + \varepsilon\ln\frac{c^3}{R^3}\ \operatorname{sgn}\dot\gamma\ .$$

Then, by imposing the yield criterion $|\sigma'_{rr}| = k$, we find that c satisfies

$$\left|\frac{c^3}{R^3} - \varepsilon\Big(1 - f_1\frac{c^3}{R^3}\Big)\right| = \left|\frac{1}{k_*}\operatorname{sgn}\,\theta_0 + \varepsilon\ln\Big(\frac{c^3}{R^3}\Big)\ \operatorname{sgn}\dot\gamma\ \right|. \quad (30)$$

Here, $\operatorname{sgn}\dot\gamma$ is determined by taking the partial time derivative of (13).

6.2.2. Simplifying features of the case $\varepsilon = 0$

According to (20b), $\varepsilon = 0$ if the phases have identical compressibilities. Because the complicating effect of differential contraction is then absent, the solution simplifies. This case is relevant for the olivine–spinel transformation: though κ_1 and κ_2 differ by about 25%, $|\varepsilon| \doteqdot 0.1$.

The solution now has the following special properties.

Within both the elastic region, and the plastic region,

$$\operatorname{sgn}\dot\gamma = \operatorname{sgn}(\theta_0\dot R). \quad (31)$$

This follows by taking the time derivative of (13).

The solution of (30) is

$$c^3 = R^3/k_*. \quad (32)$$

If the rim yields, $c > R$. This is possible if $k_* < 1$; the yield parameter $k < k_{\rm m}$. For $k_* \geq 1$, deformation is elastic.

The expression (29) for core presssure simplifies:

$$\frac{p_1}{k} = \begin{cases} (\ \operatorname{sgn}\dot\gamma)\ \ln f_1, & f_1 > k_*\,; \\ (\ \operatorname{sgn}\dot\gamma)\ \ln k_* - (1 - f_1/k_*)\operatorname{sgn}\,\theta_0, & f_1 < k_*. \end{cases} \quad (33a,b)$$

The compressibility κ now enters only through the dimensionless yield parameter k_*; otherwise (33) is identical with the corresponding relation between p_1 and f_1 for incompressible phases (Morris 2014, equation 39). Equation (33a) describes the case in which the rim is entirely plastic; (33b), that in which the core has become sufficiently small for an outer elastic region to exist.

6.2.3. Potential for $\varepsilon = 0$

In an elastic–plastic solid, part of the strain is associated with reversible distortion of the crystal lattice, part with motion of defects within the lattice. Because the former is recoverable (Hill 1950, p.26), it can be associated with a Helmholtz function F. By following the procedure given in Morris (2014, §4.1), we find that F is given by (22) above, with $|\sigma'_{rr}|$ now replaced by k when a plastic region is present.

After using the equation of state (3) to evaluate the term $p_1[V]^2_1$, we obtain

$$\Phi_2 - \Phi_1 = -[G_0]^1_2 + V_0\theta_0\, p_1 + \tfrac{1}{2}V_0|\theta_0|\frac{k^2}{k_{\rm m}}. \tag{34}$$

The definition of $k_{\rm m}$ has been used. In (34), p_1 is given by either (33a) or (33b), according as $f_1 \gtrless k_*$.

Consistent with the notation $[G_0]^2_1 = G_{02} - G_{01}$, we write $[G_0]^1_2 = G_{01} - G_{02}$ for the *positive* difference between the Gibbs functions of the parent and product phases in the initial hydrostatic state.

Let

$$\mathcal{G} = \frac{[G_0]^1_2}{V_0|\theta_0|k_{\rm m}} = (\kappa_2 + \frac{3}{4}\mu^{-1})\frac{[G_0]^1_2}{V_0\theta_0^2}, \tag{35a,b}$$

where (20a) has been used. The dimensionless parameter $\mathcal{G}$ expresses the difference $[G_0]^1_2$ of the Gibbs energies in units of strain energy per unit mass. For a given value of $[G_0]^1_2$, $\mathcal{G}$ increases with κ_2: by weakening the effect of deviatoric stress, compressibility promotes transformation.

By using the definition of $\mathcal{G}$,

$$\Phi_2 - \Phi_1 = [G_0]^1_2\Big\{ -1 + \mathcal{G}^{-1}\Big(\frac{p_1}{k_{\rm m}}\ \text{sgn}\ \theta_0 + \tfrac{1}{2}k_*^2\Big)\Big\}. \tag{35c}$$

The first term in braces represents the potential difference applied in the initial state; terms in parentheses represent the modification of that potential difference by the internal deviatoric stress.

Let

$$R_* = R/b, \qquad t_* = t/t_K\,; \qquad t_K = b/(\lambda[G_0]^1_2). \tag{36a,b,c}$$

t_K is the time taken by a sample at uniform pressure p_0 to transform completely.

Together, (35), (33) and (16) require that, for $\varepsilon = 0$,

$$\frac{{\rm d}R_*}{{\rm d}t_*} = \begin{cases} -1 + \mathcal{G}^{-1}\{\tfrac{1}{2}k_*^2 - k_*\ln R_*^3\}, & k_* < R_*^3 < 1 \\ -1 + \mathcal{G}^{-1}\{R_*^3 + \tfrac{1}{2}k_*^2 - k_*(\ln k_* + 1)\}, & R_*^3 < k_*. \end{cases} \tag{37a,b}$$

For $\mathcal{G} \to \infty$ (highly compressible rim, or vanishing rigidity, or large $[G_0]^1_2$), interface speed is uniform, and unaffected by deviatoric stress. Equation (37) holds if $k_* \le 1$; for $k_* = 1$, the entire rim deforms elastically for all $R_* < 1$. For $k_* < 1$, (37a) describes the first stage of growth: the rim is then sufficiently thin for the deformation to be everywhere plastic. In the second stage, the rim is

sufficiently thick for deformation to be elastic in its outer part; (37b) describes this stage.

According to this model, rim growth begins if the difference between the Gibbs functions of the phases in the initial hydrostatic state exceeds a critical value depending on specific volume, yield parameter, and elastic constants. Indeed, for the interface speed to be negative for $R_* = 1$, (37a) requires that $\mathcal{G} > \frac{1}{2}k_*^2$; in dimensional form,

$$[G_0]_2^1 > \begin{cases} \frac{1}{2}V_0k^2(\kappa_2 + \frac{3}{4}\mu^{-1}) & \text{for } k < |\theta_0|/(\kappa_2 + \frac{3}{4}\mu^{-1}) \\ \frac{1}{2}V_0\theta_0^2/(\kappa_2 + \frac{3}{4}\mu^{-1}) & \text{otherwise.} \end{cases}$$

Only if the yield parameter $k = 0$, so that the stress is hydrostatic, does growth start for an arbitrarily small positive value of $[G_0]_2^1$.

This property originates in the compatibility condition (10). According to it, an element of new product has been subjected to deviatoric strain during its transformation. Because, in the existing model, deviatoric stress within the product depends on the total deviatoric strain from the initial hydrostatic state, strain having occurred during transformation is manifested as stress within the fresh product. Including plasticity modifies that deviatoric stress, without eliminating it. As a result, strain energy is stored on the product side of the interface immediately upon its formation (Morris 2014, p.134). This property is not consistent with the idea that 'elastic strain energy increases continuously as the rims increase in width ... growth *eventually becomes inhibited* [emphasis added] by the accumulated strain energy' (Mosenfelder et al. 2001, p.168).

Fig.2a summarizes the behaviour predicted for purely elastic deformation. The figure is drawn for the case $\varepsilon = 0$. If $\mathcal{G} < \frac{1}{2}$, no rim forms. This is the metastable regime; within it, deviatoric stress within the rim prevents the formation of any product, even though $[G_0]_2^1 > 0$, so that product is at a lower potential than the parent phase in the initial hydrostatic state. If $\mathcal{G} > \frac{1}{2}$, the rim forms, and grows without stopping to convert the entire sample.

Fig.2b shows the effect of plasticity. In addition to allowing transformation to start for a smaller value of $\mathcal{G}$, plasticity introduces a new behaviour. Depending on the relation between $\mathcal{G}$ and k_*, rim growth may start but then stop before transformation is complete: for $\mathcal{G} > \frac{1}{2}k_*^2$, growth can start, as discussed above. Growth can, however, only continue without stopping if the maximum value of the right hand side of (37) is negative; otherwise, growth ceases before the sample is entirely transformed. The maximum occurs at $R_*^3 = k_*$; it is positive if $\mathcal{G} < \frac{1}{2}k_*^2 - k_* \ln k_* \leq \frac{1}{2}$. When growth ceases, $\mathrm{d}R_*/\mathrm{d}t_* = 0$ and

$$\mathcal{G} = \frac{1}{2}k_*^2 - k_* \ln R_*^3. \tag{38}$$

By treating k_* as a free parameter, (38) can be used to fit the existing theory to measurements of the rim thickness at which growth ceased.

By applying the corresponding equation for incompressible phases to the results of Kubo et al. (1998b), Morris (2014, §6.1) estimates the strength of wadsleyite at 13.5 GPa and 1303 K. Using (38) to include compressibility reduces the estimate by less than 10%, and the result remains consistent with

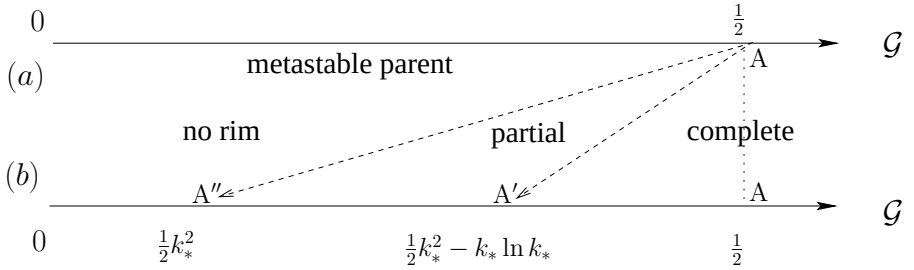

Figure 2: Behaviour predicted by existing model. For k_*, see (28); for $\mathcal{G}$, (35a). (a), $k_* = 1$ (elastic). (b), $k_* < 1$ (elastic–perfectly plastic); as $k_* \to 1$, points A', A'' coalesce with the fixed point A, and case (b) collapses to case (a).

p GPa	T K	phase	K GPa	μ GPa	ρ Mg/m^3	V_0 cm^3/mol	θ_0
15	1500	α	156[a]		3.60[a]	39.76	-0.056[e]
		β	200[b]	110[b]	3.80[b]		
18	1273	α	192[c]		3.68[a,c]	38.62	-0.067[f]
		γ	247[d]	126[d]	3.93[d]		

Table 1: Numerical values assumed for $(Mg_{0.9}Fe_{0.1})_2SiO_4$. Polymorphs: α, olivine; β, wadsleyite; γ, ringwoodite. Sources: *a*, Anderson and Isaak (1995) with 3rd order finite strain; *b*, Liu et al.(2009) with linear extrapolation; *c*, Nunez–Valdez et al. (2013); *d*, Higo et al.(2008); *e*, *f*, Rubie (1996) gives similar values $\{-0.06, -0.08\}$.

deformation experiments by Kawazoe et al.(2010) not involving phase change. (The estimate given in Morris (2014) for incompressible phases can, of course, also be obtained using (38) with the appropriate value of κ, and $\mathcal{G}$.) When the same method was applied to the ringwoodite rims in nominally anhydrous experiments (Diedrich et al. 2009; Du Frane et al. 2013), the strength was found to be 'implausibly large'. That puzzle was left unexplained (Morris 2014, §6.2).

Fig.2b provides the explanation. For those experiments, the value of $[G_0]_2^1$ is such that, if, as in Morris (2014), the phase are taken to be incompressible, $\mathcal{G}$ is only slightly less than $\frac{1}{2}$. For any transformation to occur, point A' must lie to the right of the experimental value of $\mathcal{G}$. For the experimental value of $\mathcal{G}$, this is only possible if k_* is close to unity, i.e. $k \to k_\mathrm{m}$. By setting $\kappa_2 = 0$ in (20a), we see that this requires the yield parameter $k \to \frac{4}{3}\mu|\theta_0|$. This corresponds to a stress difference comparable with the ideal strength. This explains the question left open in Morris (2014, §6.2). As we shall now see, for values of $[G_0]_2^1$ in the ringwoodite experiments, compressibility results in a value of $\mathcal{G} > \frac{1}{2}$: transformation should, according to this model, be complete, and, roughly speaking, unaffected by internal deviatoric stress.

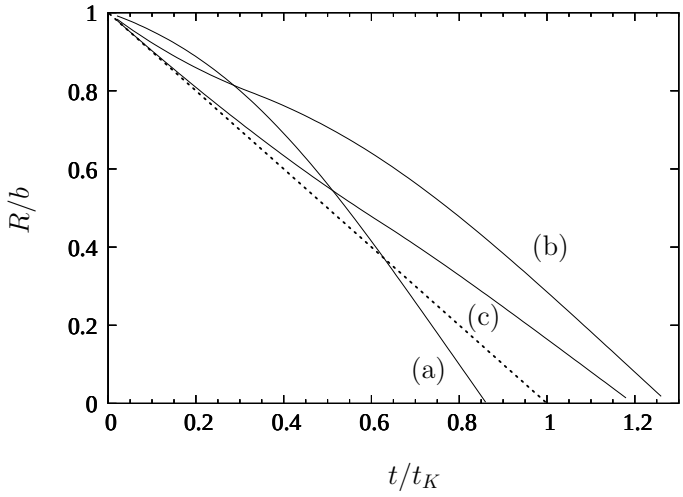

Figure 3: According to the existing model, a sample grain should transform completely at 18 GPa and 1273 K for either elastic, or elastic perfectly plastic deformation. Broken line: $\mu = 0$ (uniform sample pressure). Curve (a), Eq.(37) for $k_* = 1$ (elastic). Other curves: Eq.(37) for k_* corresponding to $|\sigma_{rr} - \sigma_{\theta\theta}|$ equalling (b) 4.75 GPa, and (c) 0.95 GPa. For t_K, see (36).

6.3. Example: rim growth for the conditions of the Du Frane experiments

For experiments at 18 GPa and 1273 K, $[G_0]_2^1 = 14.3 \pm 2.0$ kJ/mol (Mosenfelder et al. 2001), and for the material constants given in Table 1, $\mathcal{G} = 0.8$. According to Fig. 2, the rim should grow without stopping, even if deformation were perfectly elastic.

Fig.3 shows the dimensionless radius $R_* = R/b$ of the phase interface as a function of $t_* = t/t_K$. The broken line shows the solution of (37) for $\mu = 0$, corresponding to uniform pressure throughout the sample. In this case, $\mathrm{d}R/\mathrm{d}t$ is constant, and, owing to the choice (35) of timescale, R vanishes at dimensionless time $t = 1$. Curve (a) shows the solution of (37) for purely elastic deformation, with constants appropriate to the conditions of Du Frane experiments: for purely elastic strains, the interface speed is initially reduced by the deviatoric stress, but then increases with t. For $t > 0.6$ (roughly) the speed exceeds the value it would have in a sample at uniform pressure. Roughly speaking, however, we may say that above the threshold, transformation occurs at a constant speed. In §8, we shall see that this prediction is not consistent with experiment.

This behaviour results because compression work, and storage of strain energy are opposing effects. As a result, when $\mathcal{G} > \frac{1}{2}$ (i.e. outside the metastable regime), the behaviour of the transformation as whole is determined by the value of $[G_0]_2^1$, and the graph of R_* against t_* differs only slightly from that for a solid at uniform pressure.

Based on that result, we might expect plastic deformation to have little effect

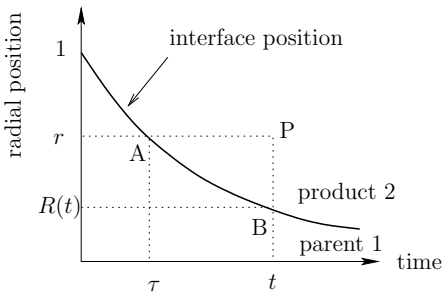

Figure 4: Sketch used to interpret the constitutive relation (7a) assumed for the product in the new model.

on the transformation time. Curves (b) and (c) confirm this expectation. The detailed shape of the graph is altered, of course. In Morris (2014), curve (e) in figure 12 shows behaviour similar to that of curves (b) and (c) in the present Fig.3. The simplicity of this outcome being a consequence of partial cancellation of strain energy storage and compression work, we should not expect it if either was absent. This leads to the new model.

7. New model

In this section, results are given only for the case $\theta_0 < 0$ (dense product).

Using Fig.4, we interpret the constitutive relation (7) for spherically–symmetric growth of a product rim. In the figure, point P represents a material element at position r; this element transformed at time τ, corresponding to point A in the figure. In (7a), the term $e'_{2ij}(\boldsymbol{x}, \tau)$ represents the deviatoric strain at a point within the product adjacent to A. Point B represents the current location of the interface. By evaluating (13) at the appropriate value of t, and recalling that σ'_{2ij} vanishes at the interface, we may express e'_{rr} at each of those points in terms of core pressure p_1 and θ_0. In general, the term $p_1(t)$ in (13) implies that σ'_{2ij} depends on the history of the transformation.

Because the aim is to show the behaviour predicted by this model, we now treat only the case $\varepsilon = 0$. As (13) then requires that $e'_{rr}(R^+) = \frac{2}{3}\theta_0$,

$$e'_{rr}(r,t) - e'_{rr}(r,\tau^+) = e'_{rr}(r,t) - \tfrac{2}{3}\theta_0. \tag{39}$$

7.1. Elastic behaviour

7.1.1. Stress

For $\varepsilon = 0$, the constitutive relation requires that

$$e'_{rr} = \frac{1}{2\mu}\sigma'_{rr} + \tfrac{2}{3}\theta_0. \tag{40}$$

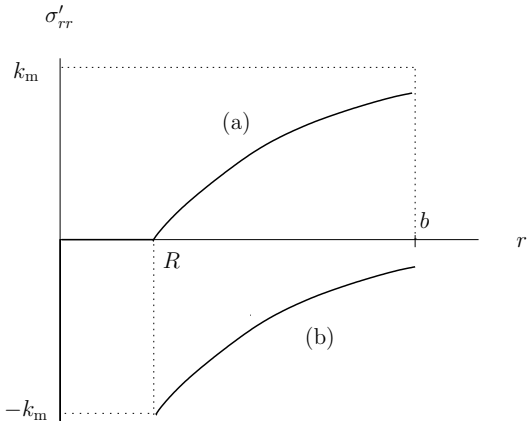

Figure 5: Radial deviatoric stress σ'_{rr} within a dense elastic rim ($\theta_0 < 0$) as a function of r. (a) new model: $\sigma'_{rr} > 0$ with greatest magnitude at $r = b$. (b) existing model: $\sigma'_{rr} < 0$ (compressive) with greatest magnitude at $r = R$.

By (40) and (13), within the product rim

$$\sigma'_{rr} = k_{\rm m}\Big(1 - \frac{R^3}{r^3}\Big). \tag{41}$$

In the new model, radial deviatoric stress is tensile; in the existing model, compressive.

Fig.5 shows the distribution of radial deviatoric stress σ'_{rr} for the two models, assuming purely elastic deformation. In the new model, the magnitude of the deviatoric stress increases with distance from the phase interface; in the existing model, it decreases.

Within the dense rim,

$$p(r) = k_{\rm m}\Big\{3\ln\frac{r}{b} + 1 - \frac{R^3}{b^3}\Big\}, \tag{42}$$

by (41), (11b) and the boundary condition $-\tilde{p} + \sigma'_{rr} = -p_0$ holding at $r = b$.

Because $\sigma'_{rr}(R^+) = 0$, p is continuous across the phase interface, and the pressure within the core is obtained by setting $r = R$ in (42). As $R \to 0$, $p_1(R) \to -\infty$. Because the absolute pressure $\tilde{p}_1 = p_0 + p_1$, the infinity in the relative pressure p means only that in this model, p_0 must be infinitely large to convert the entire sample. Indeed, it is shown below, in §7.3, that during conversion to a high–pressure phase, the absolute pressure within the core is always greater than, or equal to, the Clapeyron pressure.

Fig.6 shows the pressure distribution given by (42) with rim volume fraction f_2 as a parameter. For $f_2 \to 0$, $p \to 0$; throughout the sample, the absolute pressure $\tilde{p}$ approaches the applied pressure p_0. With increasing f_2, the minimum pressure (within the core of parent) falls increasingly below the applied pressure.

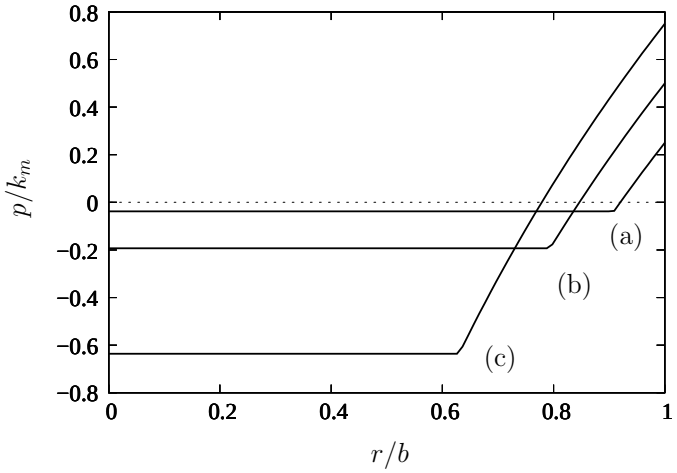

Figure 6: Dimensionless pressure as a function of position for the following values of volume fraction f_2 of product : (a) 0.25, (b) 0.5 and (c) 0.75. For $k_{\rm m}$, see (20a). Absolute pressure $\tilde{p}$ is always greater than, or equal to, the Clapeyron pressure; but, within the core, it is less than the applied pressure p_0: the relative pressure $p = \tilde{p} - p_0$ is negative within the core.

The pressure–gradient is positive, and the relative pressure p changes sign within the product rim. For any constitutive relation, the volume–averaged pressure is required by the equation of equilibrium to equal the pressure applied at the sample surface. Because, in this model, core pressure is less than the applied pressure, pressure in the outer part of the rim must exceed it, as the figure. The opposite is true in the existing model.

7.2. Plasticity

In the elastic solution, $|\sigma'_{rr}|$ increases with distance from the phase interface. As a result, deformation is elastic within a spherical shell immediately outside the phase interface. By setting $|\sigma'_{rr}| = k$ in (41), we obtain the radius of the yield surface:

$$c = R(1 - k_*)^{-1/3}. \tag{43}$$

As previously defined, $k_* = k/k_{\rm m}$. In the early stages of rim growth, the entire rim deforms elastically. As R decreases, σ'_{rr} increases in the outer part of the rim, and yielding first occurs when $c = b$; then $R = b(1 - k_*)^{1/3}$. For $k_* = 1$, the corresponding value $R = 0$; deformation is then elastic everywhere.

The radial deviatoric stress within the rim is given by

$$\sigma'_{rr} = \begin{cases} k_{\rm m}\left(1 - \frac{R^3}{r^3}\right), & R < r < c, \\ k, & c < r < b. \end{cases} \tag{44}$$

Within a dense rim, radial deviatoric stress is positive (tensile) throughout the rim.

Within the core, the absolute pressure $\tilde{p}_1$ is determined by substituting (44) into (14):

$$\frac{\tilde{p}_1 - p_0}{k_\mathrm{m}} = \begin{cases} 1 - R_*^3 + 3\ln R_*, & R_*^3 > 1 - k_*, \\ (1-k_*)\ln(1-k_*) + k_*(1 + 3\ln R_*), & R_*^3 < 1 - k_*, \end{cases} \qquad (45a,b)$$

$R_* = R/b$. For $k_* = 1$, deformation is elastic for all $R_* \neq 0$; p_1/k_m is then given by (45a) for all R_*. For $k_* < 1$, deformation is initially elastic throughout the rim; but, because stress increases with distance from the phase interface, an outer plastic region forms when the rim is sufficiently thick.

When a rim of dense product forms, $R_* \to 1$, and (45a) applies: we see that $\tilde{p}_1 - p_0$ is then negative; it is, by contrast, positive according to the existing model. When transformation is nearly complete, $R_* \to 0$, and (45b) applies: we see that $(\tilde{p}_1 - p_0)/k_\mathrm{m} \to -\infty$. This condition implies that, for complete transformation, $p_0 \to \infty$, because, as we shall see below (50), $\tilde{p}_1 \geq \bar{p}$ (Clapeyron pressure).

7.2.1. Potential

In this model of an incoherent interface, deviatoric stress is assumed to vanish within the new product at the interface. Because, for the present case of spherical symmetry, the deviatoric stress also vanishes within the core, each phase at the interface is in a hydrostatic state. The potential Φ reduces to the usual Gibbs function G from hydrostatic thermodynamics, but now evaluated at the absolute pressure $p_0 + p_1$ existing at the interface. By setting $p_1 = p_2$ in (24), and recalling that $\varepsilon = 0$, we obtain

$$\Phi_2 - \Phi_1 = [G_0]_1^2 + [V_0]_1^2\, p_1. \qquad (46)$$

According to the discussion below (24), the terms on the right side of (46) represent the Gibbs function evaluated in the hydrostatic state $\tilde{p}_1 = p_0 + p_1$. Growth ceases when $[G(\tilde{p}_1)]_2^1 = 0$. Within the core, the absolute pressure is then equal to the coexistence (Clapeyron) pressure. This result holds only for spherical symmetry: in general, it would be necessary to account for deviatoric strain energy on the parent side of the interface.

Together, (16) and (46) require that

$$\frac{\mathrm{d}R_*}{\mathrm{d}t_*} = -1 - \frac{p_1}{\mathcal{G} k_\mathrm{m}}, \qquad (47)$$

p_1 is given by (45). As defined by (36), $R_* = R/b$ and $t_* = t/t_K$. At $t_* = 0$, $R_* = 1$.

Fig.7 shows the solution of (47) for $k_* = 1$ (elastic), and conditions corresponding to the DuFrane et al. experiments at 18 GPa and 1273 K. Because results are shown for the case $\varepsilon = 0$, as curves (a) and (b), the solution is given for two different estimates of κ, the first corresponding to the compressibility of olivine and the second to ringwoodite. The solution is insensitive to the value chosen to represent κ. Curve (c) shows the solution for $\kappa = 0$, corresponding to

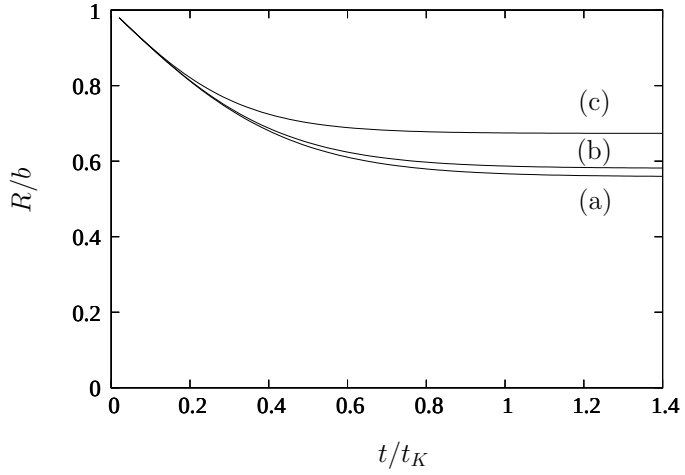

Figure 7: According to the new model, for elastic deformation, ringwoodite growth in an olivine grain will cease after a finite time at 18 GPa and 1273. For t_K, see (36). Curves, Eq. (47) for $k_* = 1$ and (a) $\kappa = 192$ GPa, (b) 247 GPa, and (c) 0 (incompressible). Other parameters, as in Table 1. For plasticity, see Fig.8. For the behaviour of the existing model at the same conditions, see Fig.3.

incompressible phases. The behaviour is similar for all three curves. Interface speed falls to zero in finite time, and rim thickness approaches an equilibrium value. The (modest) effect of plastic deformation is shown in Fig.8. This behaviour of the new model contrasts with that of the existing model (Fig.3) for identical conditions.

When growth stops, $-p_1/k_\mathrm{m} = \mathcal{G}$. By substituting for p_1, then solving for the value of R_*^3, we obtain

$$R_*^3 = \begin{cases} -W\big(-\mathrm{e}^{-1-\mathcal{G}}\big) & \text{if } \mathcal{G} < -k_* - \ln(1-k_*)\,; \\ (1-k_*)^{1-1/k_*}\mathrm{e}^{-1-\mathcal{G}/k*} & \text{if } \mathcal{G} > -k_* - \ln(1-k_*). \end{cases} \qquad (48a,b)$$

The Lambert function $W(z)$ is the solution of $W\mathrm{e}^W = z$ (dummy variable z). For $k_* = 1$, deformation is elastic, and (48a) applies for all $\mathcal{G}$. For $k_* = 0$, the stress is hydrostatic, (48b) holds for all $\mathcal{G} > 0$ and $R_*^3 = 0$.

The rim thickness x_∞ at equilibrium is obtained from (48), and the expression $x_\infty = b\{1 - R_*\}$. As shown in Fig.8, x_∞/b vanishes for $\mathcal{G} = 0$, increases continuously with $\mathcal{G}$, and approaches unity only as $\mathcal{G} \to \infty$. There is no threshold pressure: whenever $[G_0]_2^1 > 0$, some product is formed.

8. Comparison with experiment

Experiments are performed on an ensemble of geometrically similar samples cut from a single crystal of San Carlos olivine. A sample is kept at fixed temperature and pressure for a specified time. The reaction is then quenched by

reducing first the temperature, then the pressure. Because rim thickness x is measured by sectioning the sample, each value of $x(t)$ is obtained using a new sample. Kubo et al. (1998a,b) used cubes of edge length approximately 1 mm; all other authors used spheres with diameters from 425–500 μm (e.g. Diedrich et al. 2009, p.90).

In the next two figures, the observations are compared with the predicted value obtained from (48). For Fig.8, we fit values of rim thickness x measured for a given state (T, p_0 and water content) at a given time to the three–parameter function $x = c_0 + c_1 \mathrm{e}^{-c_2 t}$ (constants c_0, c_1, c_2). Because, according to this fit, $x \to c_0$ as $c_2 t \to \infty$, the constant c_0 can be compared with the predicted quantity x_∞. This is done in Fig.8, which is meant to reveal the trend in the observations. With that trend made evident, in Fig.9 the data themselves are presented and compared with the prediction of (48).

The exponential function is, of course, appropriate for cases in which transformation is complete, as well as those in which it is not. For example, in experiments on samples with 300 ppmw of water, Diedrich et al.(2009, p. 94) found that one sample transformed completely. By excluding that sample, and fitting the exponential to the remaining data in that set, we reach the same conclusion. We obtain: $c_0 = 257.5\,\mu$m, $c_1 = -251.4\,\mu$m and $c_2 = 0.0543$ min^{-1}. Because the value of c_0 exceeds the radius of even their largest spheres, samples would have transformed completely on a timescale equalling c_2^{-1}.

We use the exponential fit because the data are open to interpretation. Of their experiments at four different conditions, Kubo et al.(1998b) write that 'growth eventually ceased'. Kerschhofer et al.(1998, p.95) consider that growth ceased in three sets, but merely 'slowed considerably' in the fourth. Ambiguity arises because the sets differ in duration. Two extend to 600 minutes. For these, Kubo et al. drew curves implying that the interface velocity vanished after about 200 minutes. For the fourth set, the last measurement was made at only 200 minutes, and the authors drew a curve suggesting that the interface speed was decreasing, but still non–zero. On fitting the exponential to that set, we obtain: $c_0 = 186.2\,\mu$m, $c_1 = -141.1\,\mu$m and $c_2 = 0.0376$ min^{-1}. Though extrapolation is required, c_0 is only about one third the radius of the sphere inscribed within their cuboid samples: the fit is consistent with the statement by Kubo et al.(1998b).

In Fig.8, curves show the equilibrium rim thickness calculated from (48). Symbols show values of x_∞/b inferred from experiment. The theory provides an economic explanation of the observations. The overall trend is adequately described by curve (a) for purely elastic phases. (The two nominally dry samples are an exception, discussed below.) Curves (b), (c) show the effect of plasticity. For wadsleyite, the scale $k_\mathrm{m} = 4.5$ GPa for the numbers given in table 1, so that the value $k_* = 0.3$ used for curve (b) corresponds to $|\sigma_{rr} - \sigma_{\theta\theta}| = \frac{3}{2} k_* \, k_\mathrm{m}, = 2.0$ GPa, comparable with the value of 2–3 GPa reported by Kawazoe et al.(2010, figure 8) for a fine–grained polycrystalline wadsleyite deformed without phase change.

Though the observations are scattered around the curve for purely elastic deformation, they do not lie systematically above it. Consequently, it would not

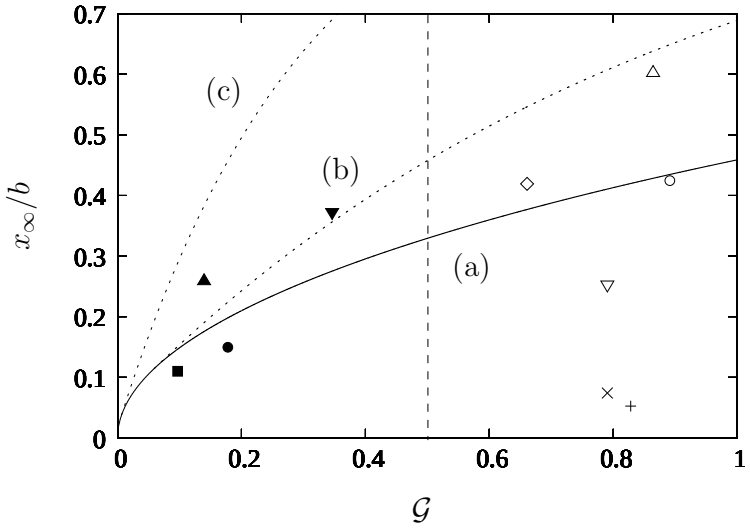

Figure 8: Equilibrium rim thickness x_∞ in units of b as a function of $\mathcal{G} = [G_0]_2^1/V_0 k_\mathrm{m}|\theta_0|$. Curves, (48) with (a) $k_* = 1$ (elastic), (b) 0.3, (c) 0.1. Vertical line, $\mathcal{G} = \frac{1}{2}$. Symbols, values inferred using an exponential fit to following data. Wadsleyite rim: Kubo et al.(1998b) 200 ppmw water, ■, 1303 K, 13.5 GPa; at 14 GPa, ●, 1403 K and ▲, 1503 K; ▼, 1603 K, 15 GPa. Mosenfelder et al.(2000) at 1373 K ◇, 16 GPa and ◯, 17 GPa. Ringwoodite rim at 18 GPa: (Diedrich et al.2009) ×, (nom.anhydrous); Du Frane et al. (2013) 75 ppmw water, ▽, 1373 K; △, 1173 K. Du Frane et al. 2013) nom. anhydrous +, 1273 K. Sample radius b in μm: 230 (Diedrich, Du Frane); 250 (Mosenfelder); 500 (Kubo, cubes modelled by the inscribed sphere).

be possible to use the yield parameter as a fitting parameter.

Curve (c) is included to show the behaviour for a lower value of the yield stress; of course, for $k_* \to 0$, $x_\infty/b \to 1$ for all $\mathcal{G} \neq 0$.

Now consider the existing model. To explain these observations, it requires the addition of separate effects, according as $\mathcal{G} \gtrless \frac{1}{2}$. As discussed in §6.3, for $\mathcal{G} > \frac{1}{2}$, the potential difference $[G_0]_2^1$ in the initial state is large enough to overwhelm the effect of internal strain energy: if the rate parameter λ were constant, all samples lying to the right of the line $\mathcal{G} = \frac{1}{2}$ should have transformed entirely. To explain why growth instead ceased, one might, for example, suggest that the reconstructive process at the interface is limited by water content over the range from < 6 ppmw (nominally anhydrous) to at least 75 ppmw, and possibly higher.[2] For $\mathcal{G} < \frac{1}{2}$, the existing model predicts metastability. As we have seen in §6.2, plastic deformation is required to explain the formation

[2]For the Mosenfelder experiments, only the water content of the starting material is known (Mosenfelder et al.2000, p.65; Mosenfelder, personal communication July 2017). Because Kubo et al.(1998a) measured 200 ppmw of water in the wadsleyite rim of a recovered sample transformed from similar material, there is no reason to expect less water in the rims of Mosenfelder et al.

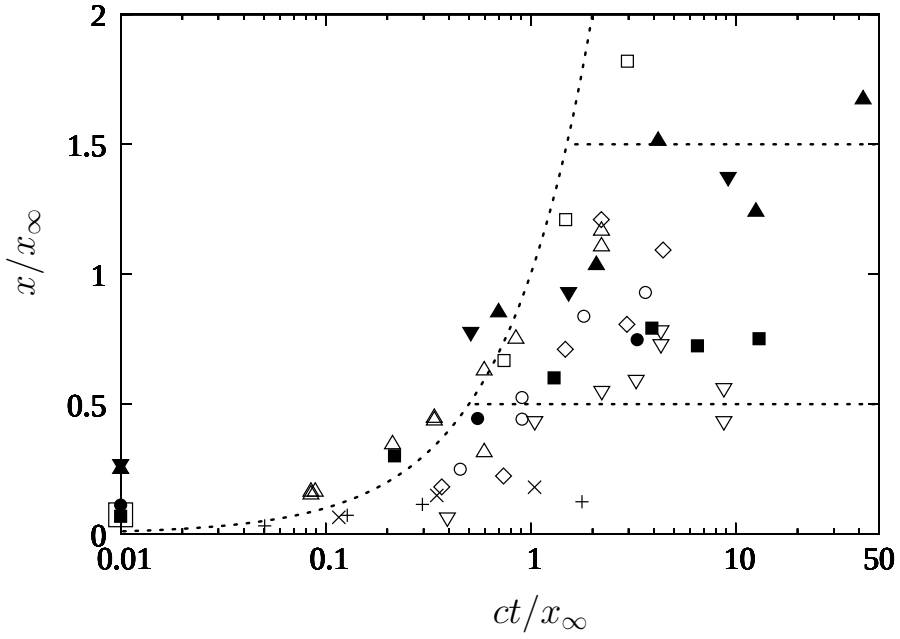

Figure 9: For 8 of 11 sets of published data, $x/x_\infty \to 1 \pm 0.5$, where x_∞ is obtained from (48) with $k_* = 1$. The exceptions are the wet series (□; 300 ppmw water; Diedrich et al.2009) in which complete transformation occurred; and two nominally anhydrous series (×, +). See text for speed c, and symbols at $ct/x_\infty = 0.01$. Broken curve, $x = ct$.

of any product at all. Using that model to explain the observations requires two additional effects, each specific to a particular range of $\mathcal{G}$. This might be considered special pleading.

Fig.9 shows measured rim thickness as a function of time. In this figure, only x_∞ is predicted. The constant c represents the interface speed at the instant when $x = 0$. It is empirical: $c = c_2\, c_0$ where c_2 and c_0 are obtained from the fit already described. In the original papers, a few data were assigned a nominal time $t = 0$; these data are shown here at $ct/x_\infty = 0.01$.

In some cases (Kubo,■) the agreement is adequate; in others (Mosenfelder, ◯), agreement is promising, but measurements are needed at longer times; in yet other cases (Du Frane, ▽), x/x_∞ first increases to about 0.75 then decreases to about 0.5. As can be seen by consulting the original papers, the non–monotonicity reflects uncertainty in the measurements.

Because these are difficult experiments, testing the new theory provides a challenge to experimentalists. Because, as noted by Du Frane et al. (2013), samples having lower water contents are prone to gain over long times, effort might, perhaps, be better placed in controlling experimental error at shorter times: with less scatter, the exponential fit would be more reliable.

In both figures, it is clear that, for the nominally anhydrous samples (×,

+), measured rim thickness is one tenth to one fifth that predicted. Product growth involves processes within the bulk phases, and within the atomically thin interphase region; and water could affect growth through either region. Mosenfelder et al.(2001) discuss the difficulties in distinguishing between those possibilities. Our results suggest a way to do so.

We have shown that, if the rate parameter in (16) were independent of time, purely elastic deformation would permit the formation of much thicker rims than are observed for the nominally anhydrous samples of Du Frane et al. and Diedrich et al. If further experiments on nominally anhydrous samples consistently produce the very thin rims seen by those authors, we might reasonably conclude that hydrogen is essential to the reconstructive process occurring within the interfacial region. By isolating that effect, our analysis would permit the effect of hydrogen on interface kinetics to be measured.

Unlike the existing model, the new model appears consistent with an observation by Vaughan et al.(1982). When the externally applied stress is nearly hydrostatic, the olivine to spinel transformation in magnesium orthogermanate Mg_2GeO_4 occurs by the mechanism of incoherent nucleation and growth. Though transformation occurs by the same mechanism when the applied stress includes a small deviatoric part $\sim$ 0.1–0.6 GPa, spinel crystals now grow preferentially in the direction of maximum compressive *external* stress. But, according to the existing model (Eq.27b), the deviatoric stress induced at the phase interface is of the order of the yield stress. It is unclear how, in the presence of that large internal stress, a smaller external stress could impose a preferred direction for growth. In the new model, that puzzle is resolved: deviatoric strain occurring as the lattice is being reconstructed should not cause deviatoric stress.

9. Conclusions

In the existing model of transformation via an incoherent intermediate state, it is implicitly assumed that the lattice records deviatoric stress experienced by a material element as it is transformed. This model predicts the existence of a threshold for the applied pressure. The threshold results from a competition between two mechanisms. First, as the phase interface passes over a material element, the element suffers a discontinuous deviatoric strain. The magnitude of this strain proves to be independent of how far the interface has propagated. Consequently, as each unit mass is transformed, the same amount of compression work must be performed to supply that strain energy. Production of that potential energy represents the fixed cost of transformation. Second, as a thin spherical shell is transformed, it contracts circumferentially. In an elastic body, this creates a hoop tension, which compresses the core of parent olivine. As a result, the core pressure exceeds the externally applied pressure. This effect promotes transformation, and competition between the effects creates the threshold.

Because the energetic cost is fixed, transformation occurs at, roughly speaking, a constant rate. This prediction of the the existing model is not consistent with experiment. Mosenfelder et al. (2000), Diedrich et al. (2009), Du Frane et

al. (2013) performed at an applied pressure exceeding the threshold: in these experiments, product growth slowed and appears to have ceased before the samples were completely transformed. Something, however, is inhibiting growth in these experiments. That fact leads to the new model.

Here, for the first time, we have argued that the character of the incoherent interface must be considered: if the lattice is, in fact, rebuilt as the interface propagates through it, deviatoric strain experienced by a material element as it is transformed can not be recorded within that element. That idea leads to the constitutive relation (8). Even without any adjustable parameters, such as a yield stress, the new model adequately predicts the final values of rim thickness for olivine single crystals containing 75–200 ppmw of water. For the nominally anydrous samples, however, measured rim thickness is much less than that predicted. Because the new model predicts that purely elastic strain permits *more* product to form than is observed experimentally, we conclude that water may be essential to lattice reconstruction.

By providing a experimental system allowing the effect of water on interface kinetics to be quantified, experiments on single crystals in which grain boundary nucleation dominates may also provide insight into the alternative process of intracrystalline nucleation of plateletes; for, according to Kerschhofer et al.(2000, p.69), transformation of the entire crystal by platelet growth occurs by propagation of an incoherent interface.

I am very grateful to Jim Casey, Mark Jellinek, Tomoaki Kubo, Arjun Narayanan and Panos Papadoulos for taking the time to review this work.

This research did not receive any specific grant from funding agencies in the public, commercial, or not–for–profit sectors.

References

[1] Anderson O.L., Isaak D.G. 1995. Elastic constants of mantle minerals at high temperature. In *Mineral physics and crystallography: a handbook of physical constants* ed. T.J. Ahrens. American Geophysical Union.

[2] Brudzinski M.R., Chen W.–P. 2005. Earthquakes and strain in subhorizontal slabs. it J. Geophys. Res. 110, B08303.

[3] Christian J.W. 1965. *The theory of transformations in metals and alloys.* Pergamon.

[4] Diedrich T., Sharp T.G., Leinenweber K., Holloway J.R. 2009. The effect of small amounts of H_2O on olivine to ringwoodite transformation growth rates and implications for subduction of metastable olivine. Chem. Geology 262, 87–99.

[5] Du Frane W.L., Sharp T.G., Mosenfelder J.L., Leinenweber K. 2013. Ringwoodite growth rates from olivine with $\sim$ 75 ppmw H_2O: metastable olivine must be nearly anhydrous to exist in the mantle transition zone. Phys. Earth. Planet. Inter. 219, 1–10.

[6] Eshelby J.D. 1961. Elastic inclusions and inhomogeneities. In *Progress in Solid Mechanics*, Vol. 2. Ed. I.N. Sneddon, R. Hill, pp. 89–140. Amsterdam: North-Holland.

[7] Fung Y.C. 1965. *Foundations of solid mechanics*. Prentice–Hall.

[8] Higo Y., Inoue T., Irifune T., Funakoshi K., Li B. 2008. Elastic wave velocities of $(Mg_{0.91}Fe_{0.09})_2SiO_4$ ringwoodite under P–T conditions of the mantle transition region. Phys. Earth Planet. Inter. 166, 167–174.

[9] Hill R. 1950. *The mathematical theory of plasticity*. Oxford.

[10] Kawazoe T., Karato S.–i., Ando J.–i., Jing Z. 2010. Shear deformation of polycrystalline wadsleyite up to 2100 K at 14–17 GPa using a rotational Drickamer apparatus. J. Geophys. Res. 115, B08208.

[11] Kerschhofer L., Dupas C., Liu M., Sharp, T.G., Durham W.B., Rubie D.C. 1998. Polymorphic transformations between olivine, wadsleyite and ringwoodite: mechanisms of intracrystalline nucleation and the role of elastic strain Mineral. Mag. 62, 617–638.

[12] Kerschhofer L., Rubie D.C., Sharp T.G., McConnell J.D.C., Dupas–Bruzek C. 2000. Kinetics of intracrystalline olivine–ringwoodite transformation. Phys. Earth Planet. Inter. 121, 59–76.

[13] Kubo T., Ohtani E., Kato T., Shinmei T., Fujino K. 1998a. Effects of water on the transformation kinetics in San Carlos olivine. Science 281, 85–87.

[14] Kubo T., Ohtani E., Kato T., Shinmei T., Fujino K., 1998b. Experimental investigation of the α–β transformation of San Carlos olivine single crystal. Phys. Chem. Miner. 26, 1–6.

[15] Larché F.C., Cahn J.W. 1973. A linear theory of thermochemical equilibrium of solids under stress. Acta Met. 21, 1051–1063.

[16] Larché F.C., Cahn J.W. 1978. Thermochemical equilibrium of multiphase solids under stress. Acta Met. 26, 1579–1589.

[17] Larché F.C., Cahn J.W. 1985. The interactions of composition and stress in crystalline solids. Acta Met. 33, 331–357

[18] Larché F.C. 1990. Coherent phase transformations. Annu. Rev. Mater. Sci. 20, 83–99.

[19] Liu M., Kerschhofer L., Mosenfelder J.L., Rubie D.C. 1998. The effect of strain energy on growth rates during the olivine–spinel transformation and implications for olivine metastability in subducting slabs. *J. Geophys. Res.* 103, 23 897–23 909.

[20] Liu W., Kung J., Li B., Nishiyama N., Wang Y. 2009. Elasticity of $(Mg_{0.87}Fe_{0.13})_2\ SiO_4$ wadsleyite to 12 GPa and 1073 K. Phys. Earth Planet. Inter. 174, 98–104.

[21] Lee J.K., Johnson W.C. 1978. Re–examination of the elastic strain energy of an incoherent ellipsoidal precipitate. Acta Met. 26, 541–545.

[22] Lee J.K.W., Tromp J. 1995. Self–induced fracture generation in zircon. J. Geophys. Res. 100, 17753–17770.

[23] Morris S. 1995. The relaxation of a decompressed inclusion. Z. angew. Math. Phys. 46, S335–S355.

[24] Morris S.J.S. 2014. Kinematics and thermodynamics of a growing rim of high–pressure phase. Phys. Earth Planet. Inter. 228, 127–143.

[25] Morris S.J.S. 2017. Interface kinetics, grain–scale deformation, and polymorphism. Annu. Rev. Earth Planet. Sci. 45, 245–269

[26] Mosenfelder J.L., Connolly J.A.D., Rubie D. C., Liu M. 2000. Strength of $(Mg,Fe)_2\ SiO_4$ wadsleyite determined by relaxation of transformation stress. Phys. Earth Planet. Inter. 120, 63–78.

[27] Mosenfelder J.L., Marton F.C., Ross C.R., Kerschhofer L., Rubie D.C. 2001. Experimental constraints on the depth of olivine metastability in subducting lithosphere. Phys. Earth Planet. Inter. 127, 165–180.

[28] Mura T. 1987. *Micromechanics of defects in solids*. Kluwer.

[29] Nabarro F.R.N. 1940. The strains produced by precipitation in alloys. Proc. R. Soc. Lond. A 175, 519–538. doi: 10.1098/rspa.1940.0072

[30] Núñez–Valdez M., Wu Z., Yu Y.G., Wentzcovitch R.M. 2013. Thermal elasticity of $(Fe_x,Mg_{1-x})_2SiO_4$ olivine and wadsleyite. Geophys. Res. Lett. 40, 290–294.

[31] Peslier A.H., Bizimis M. 2015. Water in Hawaiian peridotite minerals: a case for a dry metasomatized oceanic mantle lithosphere. Geochem. Geophys. Geosyst. 16, 1211–1232. doi:10.1002/2015GC005780.

[32] Rubie D.C. 1996. Phase transformations in the earth's mantle. In *High pressure and high temperature research on lithosphere and mantle materials, Proceedings of the international school of earth and planetary sciences* eds. M. Mellini et al., pp. 41–66.

[33] Sokolnikoff I. S. 1956. *Mathematical Theory of Elasticity*. McGraw–Hill.

[34] Sung C.–M., Burns R.G. 1978. Crystal structural features of the olivine–spinel transition. Phys. Chem. Minerals 2, 177–197.

[35] Vaughan P.J., Green H.W., Coe R.S. 1982. Is the olivine–spinel transformation martensitic? Nature 298, 357–358.

[36] Vaughan P.J., Green H.W., Coe R.S. 1984. Anisotropic growth in the olivine–spinel transformation of Mg_2GeO_4 under nonhydrostatic stress. Tectonophysics 108, 299–322.